doi:10.1016/j.jmb.2005.11.084 J. Mol. Biol. (2006) 356, 886–903

JMB

Available online at www.sciencedirect.com

SCIENCE DIRECT®

ELSEVIER

# Effects of Co-operative Ligand Binding on Protein Amide NH Hydrogen Exchange

**Vladimir I. Polshakov[1,2], Berry Birdsall[1] and James Feeney[1]***

[1]*Division of Molecular Structure, National Institute for Medical Research The Ridgeway, Mill Hill London NW7 1AA, UK*

[2]*Center for Drug Chemistry Moscow 119815, Russia*

**Corresponding author*

Amide protection factors have been determined from NMR measurements of hydrogen/deuterium amide NH exchange rates measured on assigned signals from *Lactobacillus casei* apo-DHFR and its binary and ternary complexes with trimethoprim (TMP), folinic acid and coenzymes (NADPH/$NADP^+$). The substantial sizes of the residue-specific $\Delta H$ and $T\Delta S$ values for the opening/closing events in NH exchange for most of the measurable residues in apo-DHFR indicate that sub-global or global rather than local exchange mechanisms are usually involved. The amide groups of residues in helices and sheets are those most protected in apo-DHFR and its complexes, and the protection factors are generally related to the tightness of ligand binding. The effects of ligand binding that lead to changes in amide protection are not localised to specific binding sites but are spread throughout the structure *via* a network of intramolecular interactions. Although the increase in protein stability in the DHFR.TMP.NADPH complex involves increased ordering in the protein structure (requiring $T\Delta S$ energy) this is recovered, to a large extent, by the stronger binding (enthalpic $\Delta H$) interactions made possible by the reduced motion in the protein. The ligand-induced protection effects in the ternary complexes DHFR.TMP.NADPH (large positive binding co-operativity) and DHFR.folinic acid.NADPH (large negative binding co-operativity) mirror the co-operative effects seen in the ligand binding. For the DHFR.TMP.NADPH complex, the ligand-induced protection factors result in $\Delta\Delta G_o$ values for many residues being larger than the $\Delta\Delta G_o$ values in the corresponding binary complexes. In contrast, for DHFR.folinic acid.-NADPH, the $\Delta\Delta G_o$ values are generally smaller than many of those in the corresponding binary complexes. The results indicate that changes in protein conformational flexibility on formation of the ligand complex play an important role in determining the co-operativity in the ligand binding.



*Keywords:* hydrogen exchange; dihydrofolate reductase; protein–ligand interactions; co-operative binding; NMR

## Introduction

Detailed information about fluctuations in protein structures can be obtained from studies of amide NH protection factors detected *via* NMR-determined measurements of NH hydrogen/deuterium exchange (H/D) in proteins. Such fluctuations expose some of the NH protons to the aqueous solvent, thus facilitating the NH exchange process. This approach has been shown to be useful for assessing the stability of specific hydrogen bonds within a protein, and for monitoring the effects of ligand binding.[1] For several proteins, it has been proposed that the most highly protected NH groups exchange by means of a global unfolding process.[1–7] In these cases the change in free energy $\Delta G_o$ for the opening/closing equilibrium associated with the protected amide NH has a value approaching that of the $\Delta G$ for global unfolding. However,

Abbreviations used: H/D, hydrogen/deuterium exchange; DHFR, dihydrofolate reductase; folinic acid 5-formyl-5,6,7,8-tetrahydrofolic acid; HSQC, hetero-nuclear single quantum coherence spectroscopy; NOE, nuclear Overhauser effect; NOESY, NOE spectroscopy; S.E.M., standard error of the mean; TMP, trimethoprim (2,4-diamino-5-(3,4,5-trimethoxybenzyl)pyrimidine).

E-mail address of the corresponding author: jfeeney@nimr.mrc.ac.uk

observations of different $\Delta G_o$ values (related directly to protection factors) for many NHs in a protein indicate that local and sub-global unfolding mechanisms are responsible for the exchange in most cases. The emerging picture is one where the NH exchange events take place within a complex statistical ensemble of different conformational states.[8–17] Studies of the dependence of NH exchange rates on temperature and chemical denaturant concentration,[18,19] and on hydrostatic pressure,[20] have been used to identify residues for which the exchange is controlled by local rather than global or sub-global mechanisms. Such information has been used to define regions of co-operative stability. However, Clarke and Fersht have cautioned against using this approach in isolation for determining folding pathways.[21] Several workers have discussed the implications of NH exchange studies in relation to co-operative interactions within protein structures.[14,22,23] Calculated ligand-induced NH protection factors have been used to attempt to indicate the protein structural pathway followed by the stabilising interactions accompanying ligand binding.[24] Other workers have used NH/ND exchange data to explore the origins of co-operative binding,[25–27] and to reveal details of the order of events involved in protein–DNA recognition.[28,29]

Here, we report on the NH protection factors for apo-dihydrofolate reductase (DHFR) and a series of its binary and ternary ligand complexes that are known to show binding co-operativity. DHFR is a pharmacologically important target enzyme for several antibacterial, anticancer and antimalarial drugs. These antifolate drugs often bind to the protein with large positive co-operativity in the presence of the coenzyme NADPH.[30] In the case of the antibacterial drug trimethoprim (TMP; trimethoprim(2,4-diamino-5-(3,4,5-trimethoxybenzyl)pyrimidine)), the co-operative binding has been implicated directly in the specificity of drug binding to bacterial DHFRs when compared to mammalian DHFRs.[31] Another ligand, the tetrahydrofolate analogue 5-formyl-5,6,7,8-tetrahydrofolic acid (folinic acid), binds to DHFR with strong negative co-operativity in the presence of NADPH:[32] similar negative co-operativity binding effects have important implications in the control of product release in the enzyme reaction mechanism.[33] The detailed origins of positive and negative co-operative ligand binding are still poorly understood. One possible explanation calls for the first ligand to induce conformational changes in the protein that produce an altered binding environment for the second ligand. In the present study, measurements of NH exchange protection factors for *Lactobacillus casei* DHFR, and its binary and ternary complexes with trimethoprim, folinic acid and coenzyme are examined to explore the thermodynamics of the ligand-induced conformational changes.

## Results

### NH protection factors in DHFR and its complexes

The $^{15}N$–$^{1}H$ heteronuclear single quantum coherence spectroscopy (HSQC) spectra at 15 °C and pH 6.5 of apo-DHFR dissolved in $H_2O$ and after 20 h of H/D in $^{2}H_2O$ are shown in Figure 1(a) and (b), respectively. Even at 15 °C, relatively few protein residues remain unexchanged in the $^{2}H_2O$ spectra. Most of the unchanged residues belong to amide NHs in the well-protected β-strand protein core of DHFR (the structure has an eight-stranded twisted β-sheet and four α-helices as shown in Figure 2).[34] Upon ligand binding, the amide NH groups become more protected, as seen by comparing the spectra of apo-DHFR (Figure 1(b)) with those of the DHFR.TMP and DHFR.TMP.NADPH complexes at pH 6.5 (Figure 1(c) and (d)). For apo-DHFR it was possible to measure only 50 NH resonances, whereas for the DHFR.TMP and DHFR.TMP.NADPH complexes there were 83 and 91 measured NH resonances, respectively (including some from residues in non-regular secondary structure elements).

The measurements of amide H/D rates in $^{15}N$-labelled apo-DHFR and its complexes were carried out using heteronuclear $^{15}N$–$^{1}H$ NMR spectroscopy (at 15 °C and pH 6.5) and the protection factors were determined as $\Delta G_o$ values, the Gibbs energy differences between the open and closed states (see Tables 1 and 2). The exchange rates for apo-DHFR were measured over the range 5–20 °C and the $\Delta G_o$, $\Delta H$ and $T\Delta S$ values together with the specific heat capacity difference ($\Delta C_p$) values for the opening/closing events for the individual residues were extracted from the data as described in Materials and Methods (see Table 3). The $\Delta G_o$ values measured at 15 °C and pH 6.5 for apo-DHFR and its binary and ternary complexes with TMP, folinic acid and NADPH are given in Table 1: most of the measurable protection factors ($\Delta G_o$ values) are for amide NH protons located either in or close to the well-defined secondary structure elements shown in Figure 2. Table 1 contains the ligand-induced protection factors expressed as $\Delta\Delta G_o$ values for all residues for which data for apo-DHFR and the relevant complexes are available. Similar data for the binary and ternary complexes with TMP and $NADP^+$ are given in Table 2. Bar charts indicating the ligand-induced protection factors ($\Delta\Delta G_o$ values) for all the complexes are given in Figure 3.

DHFR complexes have larger overall NH protection factors (higher $\Delta G_o$ values) than apo-DHFR, where the protected residues are mainly in the eight β-strands (strands A–H) and α-helices (C and E) (see Table 1). For the binary complexes with TMP, folinic acid, NADPH and $NADP^+$ there are substantial increases in the protein protection factors for many of the residues. The NH reso-

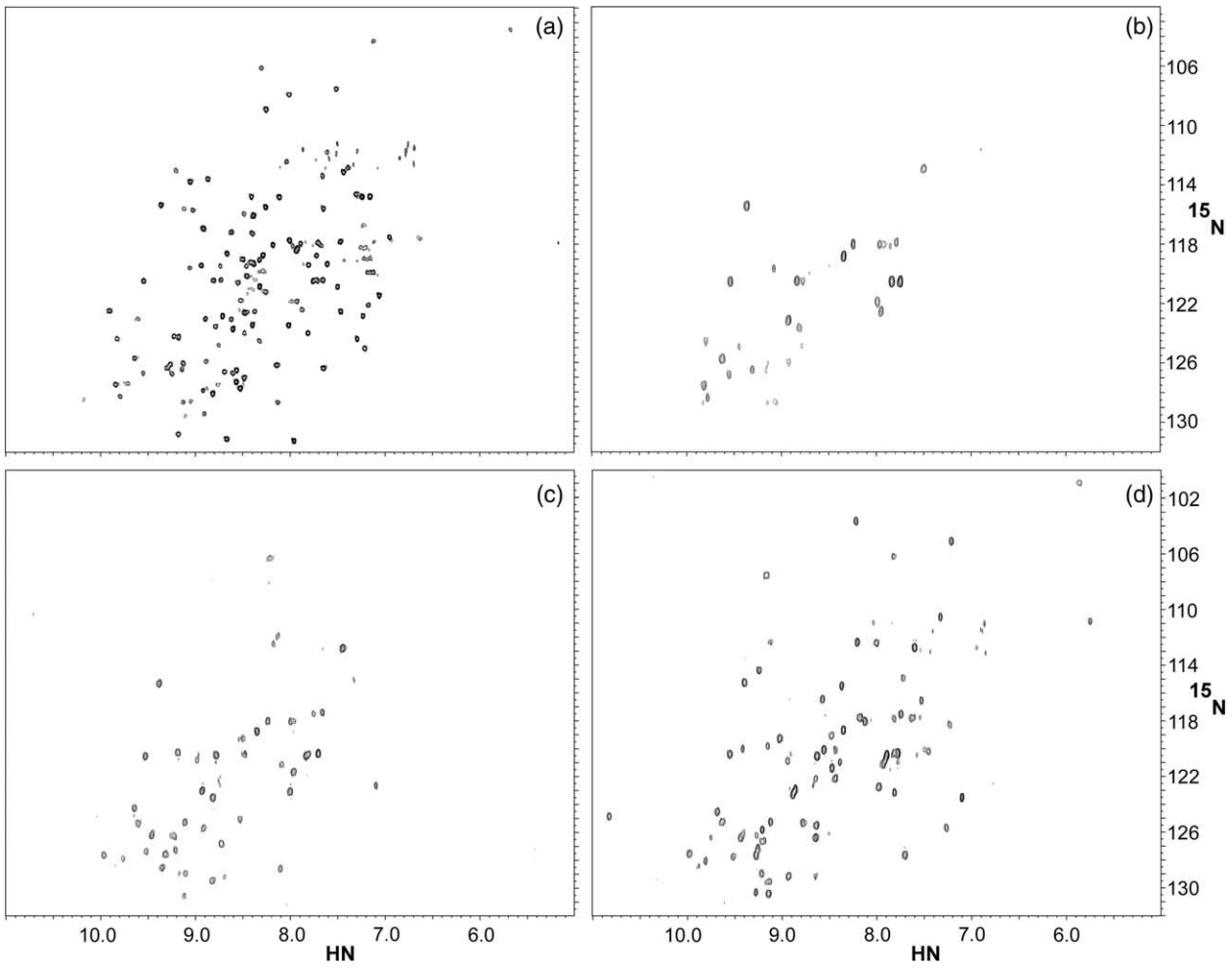


**Figure 1.** $^{15}N$–$^{1}H$ HSQC spectra of apo-DHFR dissolved in (a) $H_2O$ and (b) after 20 h of H/D in $^{2}H_2O$ at 15 °C and pH 6.5 and (c) DHFR.TMP and (d) DHFR.TMP.NADPH.

nances in the ternary complex DHFR.TMP.NADPH show the largest overall ligand protection factors (see Tables 1 and 2, and Figure 3). The individual $\Delta\Delta G_o$ value for each residue in the ternary DHFR.TMP.NADPH complex (Figure 3(a)) is usually much larger than its corresponding value in the ternary DHFR.folinic acid.NADPH complex (Figure 3(c)). The mean values of $\Delta\Delta G_o$ in the series of ternary complexes DHFR.TMP.NADPH (2.9($\pm$ 0.3) kcal mol$^{-1}$), DHFR.TMP.NADP (2.7($\pm$ 0.2) kcal mol$^{-1}$), DHFR.folinic acid.NADPH (2.1($\pm$0.2) kcal mol$^{-1}$) generally reflect the respective binding constants in the complexes (mean$\pm$ S.E.M). For the binary complexes, $NADP^+$ shows the least protection (1.7($\pm$0.2) kcal mol$^{-1}$) (Figure 3(g)). On forming all complexes, changes in protection are observed in helices and strands regardless of whether the secondary structure elements have direct interactions with the ligands.

Interestingly, many residues in the DHFR.folinic acid.NADPH ternary complex show smaller ligand protection factors compared with the corresponding values in the component binary complexes (see Table 1): this contrasts with the behaviour seen for DHFR.TMP.NADPH.

## Non-additivity of protection factors

It is seen from Tables 1 and 2 that the ligand-induced protection factors ($\Delta\Delta G_o$ values) for many residues in the ternary complexes are different from those of the sums of the values measured in the component binary complexes. Thus, the protection factor induced by a ligand, for example NADPH, is different in its binary and ternary complexes. Although several residues show protection when NADPH is added to the binary DHFR.folinic acid complex, most of the residues become less protected, indicating a destabilisation of the structure. This contrasts with the behaviour seen for the DHFR.TMP.NADPH complex (and $DHFR.TMP.NADP^+$), where the protection factors are generally increased compared with the values in the two corresponding binary complexes. This is demonstrated clearly in Figure 4, which shows a plot of the differences in $\Delta\Delta G_o$ values between ternary and binary complexes ($\Delta\Delta G_o^{\text{ternary–binary}}$) against the residue numbers (data given in Table 4): the folinic acid-containing complexes show many residues with large negative values

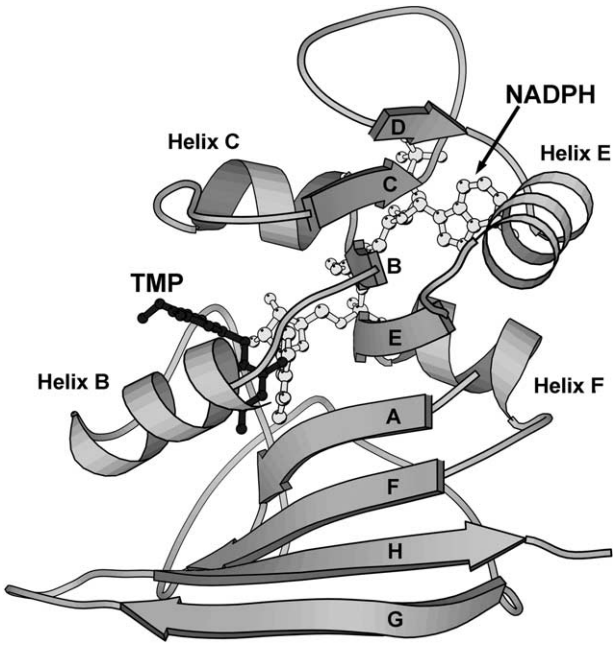


**Figure 2.** The representative NMR structure of DHFR.TMP.NADPH complex,[34] displayed using MOLSCRIPT.[60]

for $\Delta\Delta G_o^{\text{ternary–binary}}$ compared with those in the TMP-containing complexes.

### The pH-dependence of the NH exchange rates

In addition to the detailed experiments at pH 6.5 discussed above, NH exchange rates for apo-DHFR and its complexes with TMP and TMP.NADPH were also carried out at pH 7.5. For apo-DHFR, in all cases where the change in exchange rates could be measured, the values at the higher pH value were a factor of at least 10 greater than the corresponding values at pH 6.5 (see Table 3S in Supplementary Data). Had the mechanism for exchange been EX1 at pH 6.5, there would have been no change in rate with pH (assuming that the protein stability is pH-independent). For apo DHFR, the rates at pH 7.5 and pH 6.5 expressed as the ratios $k_{ex}^{7.5}/k_{ex}^{6.5}$ are in the range 11.2 to 23.8. These values are consistent with an EX2 exchange mechanism, which predicts a factor of 10 increase in rate following an increase in pH of one unit: the observed greater than tenfold increase indicates that there is also a contribution from a pH-dependent change in the stability of the protein.

For those residues in the DHFR.TMP and DHFR.TMP.NADPH complexes where only limiting values of the exchange rates could be estimated (rates too slow to measure over the timescale of our present experiments), it was not possible to assess the change in the above ratio; however, in cases where rates could be measured, the values at the higher pH were always greater than the limiting values measured at lower pH (see Supplementary Data, Table 3S). A few residues had small ratios ($<$ 4), indicating possible contributions from EX1 at pH 7.5: such values were not included in the comparisons shown in Table 4 and Figure 4.

### Temperature effect on amide backbone protection factors: residue-specific enthalpies, entropies and specific heat capacities

The effects of temperature on the NH H/D rates in apo-DHFR have been studied. Fitting the temperature-dependence of protection factors using equation (5) (see Materials and Methods) gives the residue heat capacities, $\Delta C_p$ values, entropies ($T\Delta S$) and enthalpies ($\Delta H$) for the opening processes (the values are given in Table 3 and Figure 5). These parameters correspond to the partial unfolding processes that precede the hydrogen exchange. The residue enthalpy/entropy plot for the apo-enzyme provides a good example of enthalpy/entropy compensation (see Figure 5): similar effects have been reported in NH exchange studies by other workers.[16,21,35] The observed effect is not surprising,[36] since the compensation is required to keep the $\Delta G_o$ values within the fairly narrow range of values observed for the different residues in apo-DHFR and its complexes.

Positive heat capacities ($\Delta C_p$ values) were observed for almost all measured residues in apo-DHFR. Microcalorimetric studies of protein unfolding indicate that unfolding is generally associated with positive heat capacities ($\Delta C_p$ values), and this is mirrored in the positive heat capacities for the opening/closing events in NH exchange for all the residues in the apo-DHFR.

Values of enthalpies and entropies for the openings of the individual residues for apo-DHFR were found in the ranges $\Delta H$ (7 to 35 kcal mol$^{-1}$) and $T\Delta S$ (1 to 28 kcal mol$^{-1}$). These positive values parallel those typically measured in calorimetric studies of global unfolding.

## Discussion

The largest NH protection factors are generally observed for residues in secondary structure elements such as β-sheets and α-helices (see Tables 1 and 2). For these residues, the NH exchange could take place in small populations of protein that have substantially unfolded regions present in equilibrium with more folded forms of the protein. When ligands are bound, the overall stability of the protein structure increases as indicated by the observed increased values of the NH protection factors and the increased number of residues having measurable protection factors. Ligand binding thus shifts the equilibrium towards the more folded forms of the protein resulting in an increase in the NH protection factors. The much smaller protection factors expected for residues in flexible loops are generally not detectable by the method

**Table 1.** Values of protection factors ($\Delta G_o$) and ligand-induced protection factors ($\Delta\Delta G_o$) in kcal mol$^{-1}$ measured at 15 °C and pH 6.5 for apo-DHFR and its complexes with TMP, folinic acid and NADPH

| Residue | Structural element | apo-DHFR, $\Delta G_o$ | TMP, $\Delta G_o$ | Folinic acid, $\Delta$Go | NADPH, $\Delta G_o$ | TMP. NADPH, $\Delta G_o$ | Folinic acid. NADPH, $\Delta G_o$ | TMP, $\Delta\Delta G_o$ | Folinic acid, $\Delta\Delta G_o$ | NADPH, $\Delta\Delta G_o$ | TMP. NADPH, $\Delta\Delta G_o$ | Folinic acid. NADPH, $\Delta\Delta G_o$ |
|---|---|---|---|---|---|---|---|---|---|---|---|---|
| Ala2 | βA | 9.6 | 9.9 | >10[a] | >10 | >10 | 7.9 | >0.4[b] | >0.4 | >0.4 | >0.6 | -1.7 |
| Phe3 | βA | 7.2 | >10 | 7.9 | >10 | >10 | >10 | >2.8 | 0.7 | >2.8 | >2.8 | >2.8 |
| Leu4 | βA | 7.1 | 8.7 | 8.1 | >10 | >10 | | 1.6 | 1.1 | >2.9 | >2.9 | |
| Trp5 | βA | 5.8 | >10 | >10 | 8.9 | >10 | | >4.2 | >4.2 | 3.1 | >4.2 | |
| Ala6 | βA | | >10 | >10 | 8.1 | >10 | | | | | | |
| Gln7 | βA | | >10 | 9 | >10 | >10 | | | | | | |
| Asp8 | Loop | | 7.8 | 7.7 | 7.9 | >10 | | | | | | |
| Arg9 | Loop | | 6.9 | 7.2 | 5.5 | 6.9 | 6.5 | | | | | |
| Gly11 | Loop | | 5.9 | 5.8 | 5.8 | 5.9 | 6.1 | | | | | |
| Leu12 | Loop | | | >10 | | 6 | >10 | | | | | |
| Ile13 | Loop | | >10 | >10 | | 7.5 | 7.2 | | | | | |
| Gly14 | Loop | | 6.8 | 5.9 | 7.3 | 8.2 | | | | | | |
| His18 | Loop | | | | | 7.1 | | | | | | |
| Trp21 | Loop | | 5.9 | 5.4 | 5.4 | >10 | | | | | | |
| Asp26 | αB | | 4.8 | 4.6 | | 5.1 | | | | | | |
| Leu27 | αB | | 3.6 | 4.2 | | 4.1 | | | | | | |
| His28 | αB | | | | | | | | | | | |
| Tyr29 | αB | | 5.9 | 6.7 | | 6.1 | | | | | | |
| Phe30 | αB | | >10 | >10 | | >10 | | | | | | |
| Arg31 | αB | | | 8.9 | | | 6.5 | | | | | |
| Ala32 | αB | | | 8.6 | | 6.4 | 7 | | | | | |
| Gln33 | αB | | >10 | >10 | | >10 | | | | | | |
| Thr34 | Loop | | >10 | 9 | | >10 | 6.7 | | | | | |
| Val35 | Loop | | 5.1 | 9 | | | 6.9 | | | | | |
| Lys37 | Loop | | >10 | 9.3 | | | >10 | | | | | |
| Ile38 | βB | | 5.3 | >10 | | >10 | 7 | | | | | |
| Met39 | βB | 6.7 | | 9.3 | >10 | >10 | >10 | | 2.7 | >3.3 | >3.3 | >3.3 |
| Val40 | βB | 6.3 | 8.6 | >10 | >10 | >10 | 9.1 | 2.4 | >3.7 | >3.7 | >3.7 | 2.9 |
| Val41 | βB | 6.3 | >10 | 8.1 | >10 | >10 | 7.3 | >3.7 | 1.7 | >3.7 | >3.7 | 1 |
| Gly42 | βB | 6.3 | >10 | >10 | >10 | >10 | >10 | >3.7 | >3.7 | >3.7 | >3.7 | >3.7 |
| Arg43 | αC | | | | | >10 | | | | | | |
| Arg44 | αC | | | | 7 | 7.6 | | | | | | |
| Thr45 | αC | | | | 7.9 | 7.7 | | | | | | |
| Tyr46 | αC | 5.5 | >10 | 8.2 | >10 | >10 | | >4.5 | 2.7 | >4.5 | >4.5 | |
| Glu47 | αC | 4.9 | 7.2 | 8.8 | 7.2 | >10 | | 2.3 | 4 | 2.4 | >5.1 | |
| Ser48 | αC | 5.4 | 6.5 | 7.9 | 6.9 | >10 | 7.9 | 1.1 | 2.4 | 1.5 | >4.6 | 2.4 |
| Phe49 | αC | 5.4 | >10 | 9 | 6.4 | >10 | 7.9 | >4.6 | 3.6 | 0.9 | >4.6 | 2.4 |
| Leu54 | Loop | | | 7.5 | | 4.5 | 7 | | | | | |
| Arg57 | Loop | 4.6 | 4.6 | 4.8 | 4.7 | 4.6 | 5 | 0 | 0.2 | 0.2 | 0.1 | 0.5 |
| Thr58 | βC | | | | | 6.8 | | | | | | |
| Val60 | βC | | 8.9 | | | >10 | 7.9 | | | | | |
| Val61 | βC | | | | | | | | | | | |
| Leu62 | βC | 5 | >10 | >10 | >10 | >10 | 8.2 | >5.0 | >5.0 | >5.0 | >5.0 | 3.2 |
| Thr63 | βC | 5.2 | 7.2 | 7.7 | >10 | >10 | 7.7 | 2 | 2.4 | >4.8 | >4.8 | 2.4 |
| His64 | Loop | | | | | >10 | | | | | | |

| | | | | | | | | | | | | |
|---|---|---|---|---|---|---|---|---|---|---|---|---|
| Gln65 | Loop | | | | | 7.1 | | | | | | |
| Ala73 | Loop | 4.4 | 4.6 | 6.9 | | 6.4 | 4.4 | 0.1 | 2.5 | | 2 | -0.1 |
| Val74 | βD | 6 | >10 | >10 | | | >10 | >4.0 | >4.0 | | | >4.0 |
| Val75 | βD | 3.2 | 2.8 | 3.1 | 3.3 | 3.3 | 3.5 | −0.3 | 0 | 0.1 | 0.2 | 0.3 |
| Val76 | βD | 6.2 | >10 | 8.3 | | >10 | >10 | >3.8 | 2.1 | | >3.8 | >3.8 |
| Asp78 | Loop | | | | 4.9 | 5.1 | | | | | | |
| Ala 81 | αE | | | 5.2 | | 6.2 | 4.2 | | | | | |
| Val 82 | αE | 7.9 | >10 | >10 | >10 | | | >2.1 | >2.1 | >2.1 | | |
| Phe 83 | αE | 6.5 | 6.8 | 6.5 | | 6.4 | | 0.3 | 0 | | −0.1 | |
| Ala84 | αE | 6.2 | 6 | 6.2 | 5.6 | 5.8 | 5.8 | −0.1 | 0 | −0.5 | −0.4 | −0.4 |
| Tyr85 | αE | 7 | | 9.2 | | 8.5 | >10 | | 2.2 | | 1.5 | >3.0 |
| Ala86 | αE | 7.4 | 8.4 | 7.9 | | >10 | >10 | 1 | 0.6 | | >2.6 | >2.6 |
| Lys87 | αE | 6.7 | 6.8 | 7 | 7 | 6.9 | 7.1 | 0.1 | 0.3 | 0.3 | 0.2 | 0.4 |
| Gln88 | αE | 4.7 | 4.6 | 4.6 | 4.8 | 4.7 | 4.9 | −0.2 | −0.2 | 0 | 0 | 0.2 |
| His89 | αE | 6.7 | 6.8 | 6.8 | | 7 | | 0.2 | 0.1 | | 0.3 | |
| Gln92 | loop | 4.2 | 4.2 | 4.3 | 4.5 | 4.3 | 4.8 | 0 | 0 | 0.2 | 0.1 | 0.6 |
| Leu94 | βE | 5.4 | | 5.9 | | | 5.8 | | 0.6 | | | 0.4 |
| Val95 | βE | >10 | | 9.7 | >10 | >10 | 6.9 | | <−0.3 | | | |
| Ile96 | βE | 7.7 | >10 | >10 | >10 | >10 | 7.7 | >2.3 | >2.3 | >2.3 | >2.3 | −0.1 |
| Ala97 | βE | 7.3 | >10 | 7.7 | >10 | >10 | | >2.7 | 0.3 | >2.7 | >2.7 | |
| Gly98 | Loop | 5.2 | 8.3 | 8.3 | >10 | >10 | | 3.2 | 3.1 | >4.8 | >4.8 | |
| Gly99 | Loop | | | 5.9 | 8 | 9.4 | 6.4 | | | | | |
| Ala100 | αF | | | | 6.5 | 8 | | | | | | |
| Gln101 | αF | | | | | 6.4 | | | | | | |
| Ile102 | αF | | 3.2 | | >10 | | 6.5 | | | | | |
| Phe103 | αF | 5.2 | 7.2 | 6.3 | >10 | >10 | 6.9 | 2 | 1.1 | >4.8 | >4.8 | 1.7 |
| Thr104 | αF | | 5 | 5.5 | 8.2 | 8.3 | 7.1 | | | | | |
| Ala105 | αF | | 4.5 | 5.3 | 7.2 | 7.6 | 7 | | | | | |
| Phe106 | αF | | >10 | >10 | >10 | >10 | >10 | | | | | |
| Lys107 | Loop | 5.1 | 4.8 | 5.3 | | 6 | 6.1 | −0.3 | 0.2 | | 0.9 | 1 |
| Asp111 | Loop | | | 5.5 | | | 5.4 | | | | | |
| Thr112 | βF | 6.5 | >10 | >10 | >10 | >10 | >10 | >3.5 | >3.5 | >3.5 | >3.5 | >3.5 |
| Leu113 | βF | 7.2 | >10 | 7.7 | >10 | >10 | >10 | >2.8 | 0.5 | >2.8 | >2.8 | >2.8 |
| Leu114 | βF | | >10 | | | >10 | >10 | | | | | |
| Val115 | βF | | 8.2 | 7 | 5.4 | >10 | | | | | | |
| Thr116 | βF | 5.6 | >10 | >10 | >10 | >10 | | >4.4 | >4.4 | >4.4 | >4.4 | |
| Arg117 | βF | 6.5 | >10 | | | >10 | >10 | >3.5 | | | >3.5 | >3.5 |
| Leu118 | βF | | 8.6 | >10 | >10 | >10 | 8.5 | | | | | |
| Ala119 | Loop | | 6.6 | 6.9 | 5.1 | 6.5 | 6.2 | | | | | |
| Gly120 | Loop | | 7.2 | 7 | 6.7 | | 7.6 | | | | | |
| Phe122 | Loop | | 6.2 | 5.6 | 6.4 | | 5.8 | | | | | |
| Met128 | Loop | 7.2 | 7 | 6 | 7 | 9.3 | 7 | −0.2 | −1.2 | −0.2 | 2 | −0.2 |
| Ile129 | Loop | | 7.4 | 5.9 | 6.5 | 6.7 | 6.5 | | | | | |
| Trp133 | Loop | | 5.4 | | 5.6 | | | | | | | |
| Asp135 | Loop | | 3.8 | 4.1 | | 3.7 | | | | | | |
| Phe136 | βG | 6.7 | >10 | 7.9 | 9.1 | 8.2 | 8.2 | >3.3 | 1.2 | 2.4 | 1.5 | 1.5 |
| Thr137 | βG | 7.3 | >10 | >10 | >10 | >10 | >10 | >2.7 | >2.7 | >2.7 | >2.7 | >2.7 |
| Val139 | βG | | >10 | 5.8 | | >10 | 6.2 | | | | | |
| Ser140 | βG | | 5.9 | 5.9 | 5.8 | 5.9 | 6.2 | | | | | |
| Arg142 | βG | | 6.4 | 5.8 | | 6.5 | 6.5 | | | | | |
| Val144 | βG | 4.5 | 8.5 | 8.7 | 6.8 | >10 | >10 | 4 | 4.2 | 2.3 | >5.5 | >5.5 |

(*continued on next page*)

**Table 1** (*continued*)

| Residue | Structural element | apo-DHFR, $\Delta G_o$ | TMP, $\Delta G_o$ | Folinic acid, $\Delta Go$ | NADPH, $\Delta G_o$ | TMP. NADPH, $\Delta G_o$ | Folinic acid. NADPH, $\Delta G_o$ | TMP, $\Delta\Delta G_o$ | Folinic acid, $\Delta\Delta G_o$ | NADPH, $\Delta\Delta G_o$ | TMP. NADPH, $\Delta\Delta G_o$ | Folinic acid. NADPH, $\Delta\Delta G_o$ |
|---|---|---|---|---|---|---|---|---|---|---|---|---|
| Asp146 | Loop | | 3.4 | 3.5 | | | | | | | | |
| Asn148 | Loop | | 4.8 | | | | | | | | | |
| Leu151 | Loop | 4.3 | >10 | 6.6 | 5.8 | >10 | 7.7 | >5.7 | 2.3 | 1.5 | >5.7 | 3.3 |
| Thr152 | βH | | 5.1 | 4.7 | 4.9 | 5.3 | 5.2 | | | | | |
| His153 | βH | | >10 | 9.7 | | 10.5 | 9.1 | | | | | |
| Thr154 | βH | 5.6 | 9.9 | >10 | 8.7 | >10 | 8.8 | 4.3 | >4.4 | 3.1 | >4.4 | 3.2 |
| Tyr155 | βH | 6.2 | >10 | >10 | | >10 | >10 | >3.8 | >3.8 | | >3.8 | >3.8 |
| Glu156 | βH | 6.6 | >10 | >10 | >10 | >10 | 8 | >3.4 | >3.4 | >3.4 | >3.4 | 1.4 |
| Val157 | βH | 6.2 | | >10 | >10 | >10 | >10 | | >3.8 | >3.8 | >3.8 | >3.8 |
| Trp158 | βH | 6.7 | >10 | 7.5 | >10 | >10 | 9.3 | >3.3 | 0.8 | >3.3 | >3.3 | 2.5 |
| Gln159 | βH | 7.1 | >10 | >10 | >10 | >10 | 8.5 | >2.9 | >2.9 | >2.9 | >2.9 | 1.4 |
| Lys160 | βH | 5.8 | 5.3 | 6 | 5.5 | 5.4 | 5.9 | −0.5 | 0.2 | −0.3 | −0.4 | 0 |

The standard deviations on the data are supplied in Table 1S (Supplementary Data). N-Met DHFR was used in preparing these complexes.
[a] For well-protected residues, the NH exchange is very slow and only limiting values of $\Delta G_o$ can be measured for these residues.
[b] For several residues only limiting lower values of $\Delta G_o$ could be determined: subtractions involving one such value used to give $\Delta\Delta G_o$ are indicated with the > or < signs.

used in the present work. Compared with β-sheets and α-helices, flexible loop regions have a greater capacity to exist as mixtures of different conformations, some of which will have the NH groups exposed to solvent, thus facilitating NH exchange. Such flexible loops will also be more dynamic than the regular secondary structure elements.

Independent evidence that DHFR has partially unfolded forms in its ligand complexes was provided earlier by dynamic NMR measurements of the tri-methoxybenzyl ring-flipping in complexes of DHFR and TMP,[37,38] which showed substantial transient disruptions of the protein structure during the lifetime of the complex. The rate of TMP ring-flipping (and attendant transient structure fluctuations) was reduced on coenzyme binding.

## Direct and indirect (long-range) effects of ligand binding on protection factors

The extensive data set (see Tables 1 and 2) together with the structural information available for the DHFR.TMP.NADPH complex,[34] allows us to assess the specific effects of TMP and coenzyme binding on the stability of the protein NH residues. Consideration of the effects of ligand binding on the NH protection factors for residues in α-helices and β-strands of DHFR and its complexes (see Results) reveals that the protection factors and ligand-induced stabilisation of the protein are influenced by direct and indirect effects of the ligand binding. (i) Direct effects include direct interactions of the ligands with secondary structure elements, thus linking them together and stabilising the folded form of the protein (effects seen for direct ligand interactions with helices B, C and F, and with strands A, B and F are examples of this category (see Figure 6)). Other direct effects involve interactions that immobilise a region of flexible loop near the end of a secondary structure element and result in larger NH protection factors for residues in this secondary structure element. This is seen for stabilisation of residues in helix F and strand E when TMP binds to the loop residue A97. (ii) Indirect effects involve ligand binding to site(s) remote from the protected residues that can stabilise a secondary structure element, which itself has no direct ligand interactions. This long-range stabilisation results from the remote secondary structure element interacting with another region of the protein that is stabilised directly by ligand binding. For example, β-strands G and H in the TMP and NADPH binary and ternary complexes are stabilised by their interactions with other β-strands that are themselves stabilised by direct ligand interactions. Small, but still noticeable long-range effects of ligand binding are seen for residues in all the β-strands not already stabilised by direct interactions. Helices also show these effects (the stability of helix B is affected by long-range binding effects of NADPH in the ternary complex but not in the DHFR.NADPH binary complex). This long-range stabilisation can result in residues being

**Table 2.** Values of protection factors $\Delta G_o$ and ligand induced protection factors $\Delta\Delta G_o$ in kcal mol$^{-1}$ measured at 15 °C for apo-DHFR and its complexes with TMP and NADP

| Residues | Structural element | apo-DHFR, $\Delta G_o$ | TMP, $\Delta G_o$ | NADP, $\Delta G_o$ | NADP. TMP,[a] $\Delta G_o$ | TMP, $\Delta\Delta G_o$ | NADP, $\Delta\Delta G_o$ | NADP. TMP,[a] $\Delta\Delta G_o$ |
|---|---|---|---|---|---|---|---|---|
| Ala2 | βA | | | 6.5 | | | | |
| Phe3 | βA | 6.4 | >10[b] | 6.8 | 8.1 | >3.6 | 0.4 | 1.7 |
| Leu4 | βA | 6.2 | 7.7 | 7.6 | >10 | 1.6 | 1.5 | >3.8 |
| Trp5 | βA | 6.1 | >10 | | 9.3 | >3.9 | | 3.3 |
| Ala6 | βA | | | | 9.5 | | | |
| Gln7 | βA | | >10 | 5.7 | 7.7 | | | |
| Asp8 | Loop | | 7.3 | 5.2 | 8 | | | |
| Arg9 | Loop | | 7.1 | 4.8 | 6.9 | | | |
| Gly11 | Loop | | 5.8 | 5.1 | 5.6 | | | |
| Leu12 | Loop | | | | | | | |
| Ile13 | Loop | | 6.4 | | >10 | | | |
| Gly14 | Loop | | 6.6 | | 7.1 | | | |
| His18 | Loop | | | | | | | |
| Trp21 | Loop | | 5.9 | | 7.2 | | | |
| Asp26 | αB | | 4.8 | | | | | |
| Leu27 | αB | | 3.5 | | | | | |
| Tyr29 | αB | | 5.9 | | | | | |
| Phe30 | αB | | 8.2 | | | | | |
| Arg31 | αB | | | | | | | |
| Gln33 | αB | | 7.4 | | 8.9 | | | |
| Thr34 | Loop | | 7.6 | | >10 | | | |
| Val35 | Loop | | 4.9 | | | | | |
| Lys37 | Loop | | | | | | | |
| Ile38 | βB | 5.8 | 5.1 | 5.7 | 6.2 | −0.7 | −0.2 | 0.4 |
| Met39 | βB | 6 | >10 | 8 | >10 | >4.0 | 2 | >4.0 |
| Val40 | βB | 5.8 | 8.5 | 8.1 | >10 | 2.7 | 2.4 | >4.2 |
| Val41 | βB | 5.7 | >10 | >10 | 8.9 | >4.3 | >4.3 | 3.1 |
| Gly42 | βB | 5.7 | 8 | >10 | 9.2 | 2.2 | >4.3 | 3.5 |
| Arg43 | αC | | | | | | | |
| Arg44 | αC | | | 5.6 | 6.4 | | | |
| Thr45 | αC | | | 7.8 | | | | |
| Tyr46 | αC | 5 | >10 | 7.2 | | >5.0 | 2.2 | |
| Glu47 | αC | 4.3 | 7.2 | 6.1 | 6.9 | 2.9 | 1.8 | 2.6 |
| Ser48 | αC | 5 | 6.3 | 6.5 | 7.3 | 1.3 | 1.5 | 2.4 |
| Phe 49 | αC | 5 | 8.9 | 6.3 | 8.6 | 3.9 | 1.3 | 3.7 |
| Leu54 | loop | | | | | | | |
| Arg57 | Loop | 4 | 4.3 | 4.5 | 7.9 | 0.3 | 0.5 | 3.8 |
| Val60 | βC | 4.8 | 6.4 | | 8.4 | 1.5 | | 3.6 |
| Leu62 | βC | 4.3 | 6 | >10 | >10 | 1.7 | | >5.7 |
| Thr63 | βC | 4.6 | 7.5 | | | 2.9 | | |
| His64 | Loop | | | | | | | |
| Gln65 | Loop | | | | | | | |
| Ala73 | Loop | 4 | 4.5 | 4 | | 0.4 | 0 | |
| Val74 | βD | 5.4 | 7.6 | >10 | >10 | 2.3 | >4.6 | >4.6 |
| Val75 | βD | 2.7 | 2.7 | 3.2 | 3.1 | 0 | 0.5 | 0.5 |
| Val76 | βD | 5.5 | >10 | >10 | >10 | >4.5 | >4.5 | >4.5 |
| Asp78 | Loop | | | 4.9 | 4.9 | | | |
| Ala81 | αE | 6.6 | | 7.9 | 8.5 | | 1.2 | 1.9 |
| Val82 | αE | 6.8 | >10 | >10 | >10 | >3.2 | >3.2 | >3.2 |
| Phe83 | αE | 6.1 | 6.5 | 5.7 | 6 | 0.5 | −0.4 | −0.1 |
| Ala84 | αE | 5.7 | 5.9 | 5.6 | 5.7 | 0.3 | −0.1 | 0 |
| Tyr85 | αE | 6.6 | | | | | | |
| Ala86 | αE | 6.9 | 8.3 | 9.7 | 8.3 | 1.5 | 2.9 | 1.4 |
| Lys87 | αE | 6.2 | 6.5 | 6.8 | 6.8 | 0.3 | 0.6 | 0.6 |
| Gln88 | αE | 4.2 | 4.4 | 4.7 | 4.7 | 0.2 | 0.5 | 0.4 |
| His89 | αE | 6.4 | 6.8 | 7 | 7.1 | 0.4 | 0.6 | 0.6 |
| Gln92 | Loop | 4.5 | 4.8 | 4.9 | 5 | 0.4 | 0.5 | 0.5 |
| Val95 | βE | 6.8 | >10 | 7.8 | >10 | >3.2 | 1 | >3.2 |
| Ile96 | βE | 6.6 | >10 | | | >3.4 | | |
| Ala97 | βE | 7 | >10 | >10 | >10 | >3.0 | >3.0 | >3.0 |
| Gly98 | Loop | 5.2 | 7.7 | 7.8 | >10 | 2.5 | 2.6 | >4.8 |
| Gly99 | Loop | | | | | | | |
| Ala100 | αF | | | | | | | |
| Gln101 | αF | | | | | | | |
| Ile102 | αF | | | 4.9 | | | | |
| Phe103 | αF | 6 | 6.7 | | 4.9 | 0.6 | | −1.2 |
| Thr104 | αF | | 4.8 | 6 | 7.3 | | | |
| Ala105 | αF | | 4.4 | 6 | 6.7 | | | |

(*continued on next page*)

**Table 2** (*continued*)

| Residues | Structural element | apo-DHFR, $\Delta G_o$ | TMP, $\Delta G_o$ | NADP, $\Delta G_o$ | NADP.TMP,[a] $\Delta G_o$ | TMP, $\Delta\Delta G_o$ | NADP, $\Delta\Delta G_o$ | NADP.TMP,[a] $\Delta\Delta G_o$ |
|---|---|---|---|---|---|---|---|---|
| Phe106 | αF | 5.1 | 8.1 | >10 | | 3 | >4.9 | |
| Lys107 | Loop | 4.1 | 4.5 | 5.5 | | 0.4 | 1.4 | |
| Thr112 | βF | 6 | 7.1 | 7.3 | >10 | 1 | 1.3 | >4.0 |
| Leu113 | βF | 7 | 8.4 | 8.7 | >10 | 1.4 | 1.7 | >3.0 |
| Leu114 | βF | 5.6 | >10 | 7.4 | >10 | >4.4 | 1.8 | >4.4 |
| Val115 | βF | | 8.8 | 6.6 | 6 | | | |
| Thr116 | βF | 5.2 | 8.1 | | >10 | 2.9 | | >4.8 |
| Arg117 | βF | 5.7 | >10 | 7.2 | | >4.3 | 1.5 | |
| Leu118 | βF | | 8 | 5.2 | | | | |
| Ala119 | Loop | | 6.4 | 4.2 | 6.3 | | | |
| Gly120 | Loop | | 7.4 | 4.9 | 8.5 | | | |
| Phe122 | Loop | | 6.1 | | 6.7 | | | |
| Thr126 | Loop | | | | | | | |
| Met128 | Loop | 6.7 | 6.6 | | | −0.1 | | |
| Ile129 | Loop | | 6.7 | | | | | |
| Asp135 | Loop | | 3.6 | | 5.4 | | | |
| Phe136 | βG | 6.4 | 7.7 | 7.9 | 7.3 | 1.2 | 1.4 | 0.8 |
| Thr137 | βG | 7 | 9.1 | 8.8 | >10 | 2.1 | 1.8 | >3.0 |
| Val139 | βG | 5.3 | 6 | | | 0.7 | | |
| Ser140 | βG | 5.8 | 5.8 | 5.4 | 6.6 | −0.1 | −0.4 | 0.8 |
| Arg142 | βG | 5 | 6.2 | 6.3 | 6.3 | 1.2 | 1.2 | 1.2 |
| Val144 | βG | 4 | 8.9 | 5.7 | 8.8 | 4.8 | 1.6 | 4.7 |
| Asp146 | Loop | | 3.5 | | | 3.5 | | |
| Asn148 | Loop | | | | | | | |
| Leu151 | Loop | 3.9 | 7.4 | 5.3 | 8.2 | 3.6 | 1.4 | 4.3 |
| Thr152 | βH | 3.4 | 4.9 | 4.6 | 5.2 | 1.5 | 1.2 | 1.8 |
| His153 | βH | 7.5 | 9.8 | 6.7 | >10 | 2.4 | −0.8 | >2.6 |
| Thr154 | βH | 5.2 | 9.7 | 7 | >10 | 4.5 | 1.8 | >4.8 |
| Tyr155 | βH | 5.9 | >10 | | >10 | >4.1 | | >4.1 |
| Glu156 | βH | 6.5 | 8.3 | >10 | 7.9 | 1.8 | >3.5 | 1.4 |
| Val157 | βH | 6.1 | >10 | >10 | >10 | >3.9 | >3.9 | >3.9 |
| Trp158 | βH | 6.6 | 7.9 | 7.3 | >10 | 1.3 | 0.7 | >3.4 |
| Gln159 | βH | 6.8 | >10 | >10 | >10 | >3.2 | >3.2 | >3.2 |
| Lys160 | βH | 5.5 | 5.2 | 5.5 | 5.8 | −0.3 | 0 | 0.3 |

Non N-Met DHFR was used in preparing these complexes.

[a] The ternary complex DHFR.TMP.NADP$^+$ exists as a mixture of two distinct interconverting forms (Forms I and II) present with approximately equal populations.[61] Although several amide NHs appear as two signals, the NH exchange measurements only yield averaged protection factors because exchange between the two forms results in the signals in each pair exchanging at the same rate.

[b] For well-protected residues, the NH exchange is very slow and only limiting values of $\Delta G_o$ can be measured for these residues. The standard deviations on the data are supplied in Table 2S (Supplementary Data).

protected by a ligand that is binding on the opposite side of the protein. For strands in a β-sheet, the network of hydrogen bonds provides an obvious way of transmitting such long-range effects that can result in a decrease in the fraction of partially disrupted open structures and lead to an increase in NH stabilisation. For helices, other interactions can be used for long-range stabilisation of the structure: helix B, for example, interacts directly with helix C (*via* side-chain interactions between F30 and F49) and helix C has direct interactions with NADPH.

## Residue-specific enthalpy, entropy and specific heat capacity values

The enthalpy change on protein unfolding has been attributed to the balance between the energy involved in breaking the internal protein interactions present in the native state (such as hydrogen bonds, electrostatic interactions and van der Waals interactions) and the competing energy changes upon hydration of protein groups exposed by unfolding.[12,16,39] The entropy change accompanying protein unfolding results from the trade-off between the energy gained by increasing the conformational disorder and the energy lost in reducing the degree of freedom of water molecules solvating exposed protein surfaces in the unfolded protein.[40] The corresponding enthalpy and entropy changes ($\Delta H$ and $T\Delta S$ values) for opening/closing events in amide NH hydrogen exchange are local quantities for specific residues but they will have similar origins to those described above for protein unfolding.

The large range of residue-specific $\Delta H$ and $T\Delta S$ values observed for apo-DHFR (see Table 3 and Figure 5) indicates that there is a wide variety of conformational fluctuations leading to NH exchange for the different residues extending from local to near-global mechanisms. Sadqi and co-

**Table 3.** The thermodynamic parameters for the protection factors for NH exchange in apo-DHFR (non-Met-0 form) at 15 °C and pH 6.5

| Residues | $\Delta G_o$ (kcal mol$^{-1}$) | $\Delta C_p$ (kcal mol$^{-1}$) | $\Delta H$ (kcal mol$^{-1}$) | $T\Delta S$ (kcal mol$^{-1}$) |
|---|---|---|---|---|
| Phe3 | 6.4 | 2.9 | 21.8 | 15.5 |
| Leu4 | 6.2 | 0.7 | 20.1 | 13.9 |
| Trp5 | 6.1 | 3.5 | 26.4 | 20.3 |
| Ile38 | 5.8 | 4.4 | 19.1 | 13.3 |
| Met39 | 6.0 | 0.8 | 23.7 | 17.6 |
| Val40 | 5.8 | 1.5 | 27.6 | 21.8 |
| Gly42 | 5.7 | 0.8 | 21.2 | 15.5 |
| Tyr46 | 5.0 | 1.6 | 17.2 | 12.2 |
| Ser48 | 5.0 | 0.8 | 9.6 | 4.7 |
| Phe49 | 5.0 | 1.0 | 9.8 | 4.8 |
| Arg57 | 4.0 | 0.4 | 8.2 | 4.2 |
| Val60 | 4.8 | 0.9 | 14.1 | 9.3 |
| Val61 | 4.4 | 0.6 | 17.5 | 13.1 |
| Leu62 | 4.3 | 0.9 | 17.1 | 12.7 |
| Thr63 | 4.6 | 0.8 | 14.4 | 9.8 |
| Ala73 | 4.0 | 0.7 | 8.0 | 4.0 |
| Val74 | 5.4 | −0.9 | 28.3 | 23.0 |
| Val75 | 2.7 | 0.3 | 7.5 | 4.8 |
| Val76 | 5.5 | 1.0 | 28.0 | 22.5 |
| Phe83 | 6.1 | 0.8 | 21.6 | 15.5 |
| Ala86 | 6.9 | −2.3 | 34.8 | 27.9 |
| Gln88 | 4.2 | 1.0 | 10.7 | 6.5 |
| His89 | 6.4 | 0.5 | 14.0 | 7.5 |
| Gln92 | 4.5 | 1.0 | 15.0 | 10.6 |
| Phe103 | 6.0 | 1.9 | 12.4 | 6.3 |
| Leu113 | 7.0 | 1.1 | 31.0 | 24.0 |
| Thr116 | 5.2 | 1.5 | 21.4 | 16.2 |
| Arg117 | 5.7 | −1.2 | 6.5 | 0.8 |
| Phe136 | 6.4 | −2.6 | 28.0 | 21.5 |
| Thr137 | 7.0 | 1.0 | 27.9 | 20.9 |
| Val139 | 5.3 | −0.9 | 13.7 | 8.4 |
| Val144 | 4.0 | 1.7 | 23.3 | 19.3 |
| Leu151 | 3.9 | 1.4 | 21.2 | 17.3 |
| Thr152 | 3.4 | 2.1 | 18.5 | 15.1 |
| Thr154 | 5.2 | 0.8 | 15.6 | 10.4 |
| Tyr155 | 5.9 | 1.1 | 19.0 | 13.2 |
| Glu156 | 6.5 | 4.9 | 28.2 | 21.7 |
| Gln159 | 6.8 | 1.7 | 25.6 | 18.8 |
| Lys160 | 5.5 | 0.4 | 6.5 | 1.0 |

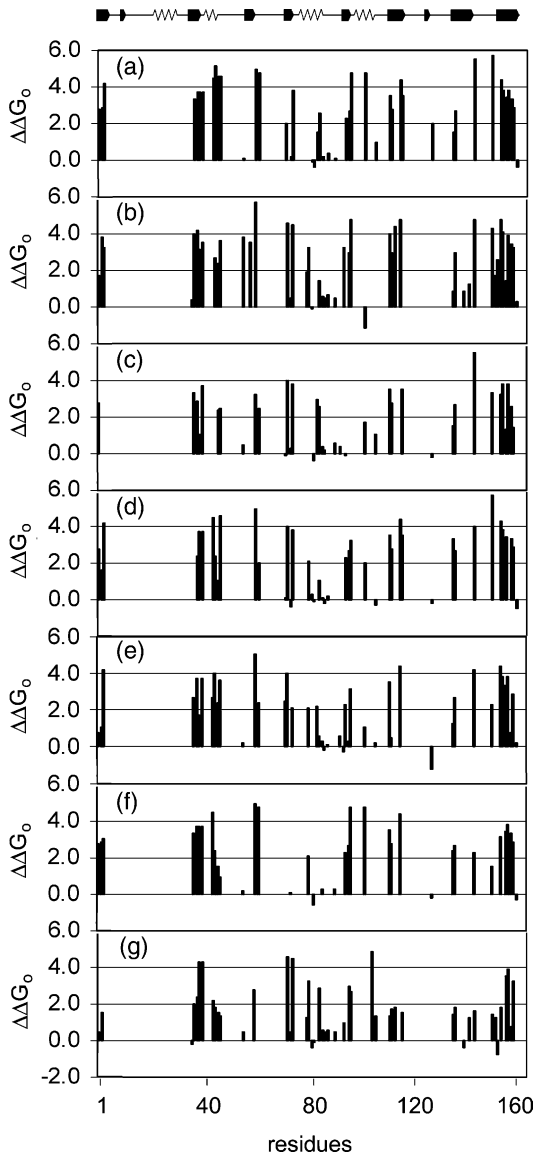


**Figure 3.** Bar charts showing the ligand-induced NH protection factors ($\Delta\Delta G_o$ in kcal mol$^{-1}$) at 15 °C and pH 6.5 for the complexes (a) DHFR.TMP.NADPH; (b) DHFR.TMP.NADP$^+$; (c) DHFR.folinic acid.NADPH; (d) DHFR.TMP; (e) DHFR.folinic acid; (f) DHFR.NADPH; and (g) DHFR.NADP$^+$.

workers have reported similar results in NH exchange studies of SH3.[16] They suggested that residues with very low values of enthalpy and entropy for NH exchange can be considered to exchange *via* local mechanisms that do not require major disruption of the protein structure: residues with medium to high values of enthalpy and entropy changes require sub-global or global disruption of the protein structure.[16] Thus, the $\Delta H$ and $T\Delta S$ values can be considered as providing information similar to that described earlier by Englander and others,[18–20] who determined when local exchange mechanisms were operating by studying the effects of chemical denaturant concentration, temperature and hydrostatic pressure on NH protection factors. The substantial sizes of the $\Delta H$ and $T\Delta S$ values for most of the measurable residues in apo-DHFR suggest that sub-global or global rather than local exchange mechanisms are usually involved. However, because our thermodynamic analysis assumes the presence of only two states rather than the ensemble of states actually present (in any unfolding equilibrium), such a strict interpretation of the $\Delta H$ and $T\Delta S$ values might not be appropriate. More definitive conclusions about the involvement of local exchange mechanisms would require extensive studies of the effects of chemical denaturation on the NH exchange rates for the apo-enzyme and its complexes.[18,19]

There is no obvious clustering of similar enthalpy and entropy values in different secondary structure elements in apo-DHFR.

The $\Delta G_o$ and $\Delta C_p$ (specific heat) values, obtained from residue-specific NMR measurements, are local quantities, in contrast to similar parameters that can be measured for global protein unfolding using techniques such as differential scanning calorime-

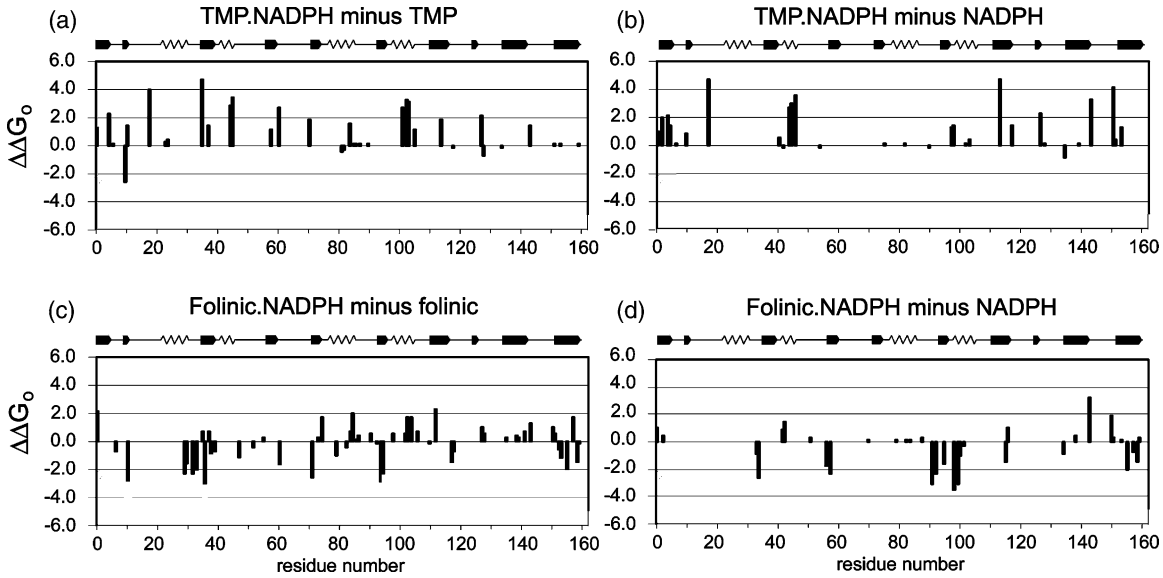


**Figure 4.** Bar charts showing the differences in ligand-induced NH protection factors between ternary and binary complexes ($\Delta\Delta G_o^{\text{ternary–binary}}$ in kcal mol$^{-1}$) at 15 °C and pH 6.5 for (a) DHFR.TMP.NADPH minus DHFR.TMP; (b) DHFR.TMP.NADPH minus DHFR.NADPH; (c) DHFR.folinic acid.NADPH minus DHFR.folinic acid; (d) DHFR.folinic acid. NADPH minus DHFR.NADPH.

try. Residues that exchange only upon global unfolding will have $\Delta G_o$ for the opening process similar to those for global unfolding. In most cases, the NMR-measured residue-specific thermodynamic parameters will be smaller than parameters obtained for global unfolding. Such differences will occur when the exchange takes place following local subunit unfolding rather than global unfolding.

For apo-DHFR, the values of the residue-specific heat capacities ($\Delta C_p$ values) are positive in agreement with the positive heat capacities typically observed for global protein unfolding[41] measured by microcalorimetry (calorimetrically determined values for the global unfolding of *L. casei* DHFR are not available).

## Ligand-induced protection factors and co-operativity of ligand binding

It is seen from Tables 1 and 2 that for most residues, the ligand-induced protection factors result in the $\Delta G_o$ values in the DHFR.TMP.NADPH ternary complex (large positive co-operativity of 135) being larger than the $\Delta G_o$ values measured in either of the component binary complexes. Similar results are seen for the DHFR.TMP.NADP$^+$ ternary complex (nearly neutral co-operativity) although the differences in $\Delta G_o$ are generally smaller. In contrast, in the case of the ternary DHFR.folinic acid.NADH complex (large negative co-operativity of 600), the $\Delta G_o$ values are often smaller than the value in at least one of the corresponding binary complexes. These dramatic differences in $\Delta G_o$ values ($\Delta\Delta G_o^{\text{(ternary–binary)}}$) for the ternary complexes are observed for residues widely spread throughout the structure and are illustrated by Figure 4. Could these differences in ligand-induced stability be related to positive and negative co-operative binding? In fact, for the three co-operative systems examined here, there is a significant linear positive correlation between the mean values of the $\Delta\Delta G_o^{\text{(ternary–binary)}}$ (obtained from data in Table 4) and log co-operativity ($r^2 = 0.89$, slope $0.32 \pm 0.06$, significantly different from zero, $P < 0.005$).

Kinetic studies have indicated that the increased binding of the TMP and NADPH ligands in the ternary complex is associated with decreased dissociation rate constants for the ligands.[42] Thus, the off-rate of one ligand is decreased when the other ligand is bound to the protein (the ternary complex being more rigid and less flexible than the binary complex). Although $T\Delta S$ energy will be lost in stabilising the protein structure, the enthalpic contributions to the ligand binding appear to be increased favourably in this more rigid form, such that they more than compensate for the entropic penalty. Williams and co-workers have already drawn attention to such effects in the ligand-induced co-operative dimerisation of the antibiotic vancomycin and in other studies involving ligands binding to streptavidin and to haemoglobin.[25–27] In the positive co-operative binding case of vancomycin, they propose that the ligand binding causes contractions of parts of the vancomycin structure, resulting in reduced chain motions that help to strengthen the hydrogen bonds between the vancomycin monomers by reducing motions that would oppose bonding.

Our results for the DHFR.TMP.NADPH complex (strongly positive co-operative binding,[42] and large positive values of $\Delta\Delta G_o^{\text{(ternary–binary)}}$ for many resi-

**Table 4.** Differences in ligand-induced NH protection factors between ternary and each of its binary complexes ($\Delta\Delta G_o^{ternary-binary}$ in kcal mol$^{-1}$) at 15 °C and pH 6.5 for DHFR.TMP.NADPH, DHFR.folinic acid.NADPH and DHFR.TMP.NADP$^+$

| Residue | Structural element | TMP.NADPH minus NADPH | TMP.NADPH minus NADPH | Folinic acid. NADPH minus folinic | Folinic acid. NADPH minus NADPH | NADP.TMP minus TMP | NADP.TMP minus NADP |
|---|---|---|---|---|---|---|---|
| Ala2 | βA | 0.4 | | $<-2.1$[a] | $<-2.1$ | | |
| Phe3 | βA | | | $>2.1$ | | $<-1.9$ | 1.3 |
| Leu4 | βA | $>1.3$ | | | | $>2.3$ | $>2.4$ |
| Trp5 | βA | | $>1.1$ | | | $<-0.7$ | |
| Ala6 | βA | | $>1.9$ | | | | |
| Gln7 | βA | | | | | $<-2.3$ | 2 |
| Asp8 | Loop | $>2.2$ | $>2.1$ | | | 0.7 | 2.8 |
| Arg9 | Loop | 0.1 | 1.5 | $-0.7$ | 1 | $-0.2$ | 2.1 |
| Gly11 | Loop | 0 | 0.1 | | 0.4 | $-0.1$ | 0.5 |
| Ile13 | Loop | $<-2.5$ | | $<-2.8$ | | $>3.6$ | |
| Gly14 | Loop | 1.5 | 0.9 | | | 0.6 | |
| Trp21 | Loop | $>4.1$ | $>4.6$ | | | 1.3 | |
| Asp26 | αB | 0.3 | | | | | |
| Leu27 | αB | 0.5 | | | | | |
| Arg31 | αB | | | $-2.3$ | | | |
| Ala32 | αB | | | $-1.6$ | | | |
| Gln33 | αB | | | | | 1.5 | |
| Thr34 | Loop | | | $<-2.2$ | | $>2.4$ | |
| Val35 | Loop | | | $-2$ | | | |
| Lys37 | Loop | | | $>0.7$ | | | |
| Ile38 | βB | $>4.7$ | | $-3$ | | 1.1 | 0.6 |
| Met39 | βB | | | $>0.7$ | | | $>2.0$ |
| Val40 | βB | $>1.4$ | | $<-0.9$ | $<-0.9$ | $>1.5$ | $>1.9$ |
| Val41 | βB | | | $-0.7$ | $<-2.7$ | $-1.1$ | $<-1.1$ |
| Gly42 | βB | | | | | 1.3 | $<-0.8$ |
| Arg44 | αC | | 0.5 | | | | 0.8 |
| Thr45 | αC | | $-0.2$ | | | | |
| Glu47 | αC | $>2.8$ | $>2.8$ | | | $-0.3$ | 0.8 |
| Ser48 | αC | $>3.5$ | $>3.1$ | 0 | 0.9 | 1 | 0.8 |
| Phe49 | αC | | $>3.6$ | $-1.2$ | 1.5 | $-0.3$ | 2.3 |
| Leu54 | Loop | | | $-0.5$ | | | |
| Arg57 | Loop | 0 | $-0.1$ | 0.2 | 0.3 | 3.5 | 3.3 |
| Val60 | βC | $>1.1$ | | | | 2 | |
| Leu62 | βC | | | $<-1.8$ | $<-1.8$ | $>4.0$ | |
| Thr63 | βC | $>2.8$ | | 0 | $<-2.3$ | | |
| Ala73 | Loop | 1.8 | | $-2.6$ | | | |
| Val74 | βD | | | | | $>2.4$ | |
| Val75 | βD | | 0 | 0.3 | 0.2 | 0.4 | 0 |
| Val76 | βD | | | $>1.7$ | | | |
| Asp78 | Loop | | 0.1 | | | | 0 |
| Ala81 | αE | | | $-1$ | | | 0.6 |
| Phe83 | αE | $-0.4$ | | | | $-0.5$ | 0.3 |
| Ala84 | αE | $-0.3$ | 0.1 | $-0.4$ | 0.1 | $-0.2$ | 0.1 |
| Tyr85 | αE | | | $>0.8$ | | | |
| Ala86 | αE | $>1.6$ | | $>2.1$ | | 0 | $-1.4$ |
| Lys87 | αE | 0.1 | 0 | 0.2 | 0.1 | 0.3 | 0 |
| Gln88 | αE | 0.2 | 0 | 0.4 | 0.2 | 0.2 | 0 |
| His89 | αE | 0.2 | | | | 0.3 | 0.1 |
| Gln92 | Loop | 0.1 | $-0.2$ | 0.6 | 0.4 | 0.1 | 0 |
| Leu94 | βE | | | $-0.2$ | | | |
| Val95 | βE | | | $-2.8$ | $<-3.1$ | | $>2.2$ |
| Ile96 | βE | | | $<-2.3$ | $<-2.3$ | | |
| Gly98 | Loop | | | | | $>2.3$ | $>2.2$ |
| Gly99 | Loop | | 1.3 | 0.6 | $-1.6$ | | |
| Ala100 | αF | | 1.4 | | | | |
| Ile102 | αF | | | | $<-3.5$ | | |
| Phe103 | αF | $>2.8$ | | 0.6 | $<-3.1$ | $-1.8$ | |
| Thr104 | αF | 3.3 | 0.1 | 1.7 | $-1$ | 2.6 | 1.3 |
| Ala105 | αF | 3.2 | 0.4 | 1.7 | $-0.2$ | 2.3 | 0.7 |
| Lys107 | Loop | 1.2 | | 0.8 | | | |
| Asp111 | Loop | | | $-0.1$ | | | |
| Thr112 | βF | | | | | $>2.9$ | $>2.7$ |
| Leu113 | βF | | | $>2.3$ | | $>1.6$ | $>1.3$ |
| Leu114 | βF | | | | | | $>2.6$ |
| Val115 | βF | $>1.8$ | $>4.6$ | | | $-2.8$ | $-0.6$ |
| Thr116 | βF | | | | | $>1.9$ | |
| Leu118 | βF | | | $<-1.5$ | $<-1.5$ | | |

(*continued on next page*)

**Table 4** (*continued*)

| Residue | Structural element | TMP.NADPH minus NADPH | TMP.NADPH minus NADPH | Folinic acid. NADPH minus folinic | Folinic acid. NADPH minus NADPH | NADP.TMP minus TMP | NADP.TMP minus NADP |
|---|---|---|---|---|---|---|---|
| | | | | | | | (*continued on next page*) |
| Ala119 | Loop | −0.1 | 1.4 | −0.8 | 1.1 | −0.1 | >2.1 |
| Met128 | Loop | 2.2 | 2.2 | 1 | 0 | | |
| Ile129 | Loop | −0.7 | 0.2 | 0.6 | −0.1 | | |
| Asp135 | Loop | −0.1 | | | | 1.8 | |
| Phe136 | βG | | −0.9 | 0.3 | −0.9 | −0.4 | −0.6 |
| Thr137 | βG | | | | | >0.9 | >1.2 |
| Val139 | βG | | | 0.4 | | | |
| Ser140 | βG | 0 | 0.1 | 0.3 | 0.4 | 0.9 | 1.2 |
| Arg142 | βG | 0.1 | | 0.7 | | 0.1 | 0 |
| Val144 | βG | >1.5 | >3.2 | >1.3 | 3.2 | −0.1 | 3.1 |
| Leu151 | Loop | | >4.2 | 1.1 | 1.9 | 0.7 | 2.9 |
| Thr152 | βH | 0.2 | 0.4 | 0.5 | 0.3 | 0.2 | 0.5 |
| His153 | βH | | | −0.5 | | >0.2 | >3.3 |
| Thr154 | βH | >0.1 | >1.3 | <−1.2 | 0.1 | >0.3 | >3.0 |
| Glu156 | βH | | | <−2.0 | <−2.0 | −0.4 | <−2.1 |
| Trp158 | βH | | | 1.7 | <−0.7 | >2.1 | >2.7 |
| Gln159 | βH | | | <−1.5 | <−1.5 | | |
| Lys160 | βH | 0.1 | −0.1 | −0.1 | 0.3 | 0.6 | 0.3 |

[a] For several residues only limiting lower values of $\Delta G_o$ could be determined: subtractions involving one such value used to give $\Delta\Delta G_o$ are indicated with the > or < signs.

dues) are consistent with the ternary complex having a tighter, less flexible structure than the binary complexes. For the DHFR.TMP.NADP$^+$ complex (with neutral co-operative binding) intermediate stabilisation is observed.

Williams and co-workers have suggested that negative binding co-operativity would be associated with expansion of part of the receptor and a corresponding decrease in NH exchange stability.[25–27] Our NH H/D results for the binary and ternary complexes of DHFR with folinic acid and NADPH support this picture. For the DHFR.folinic acid.NADPH complex, where there is strong negative co-operative binding, many of the residues have substantial negative $\Delta\Delta G_o^{(\text{ternary–binary})}$ values fully consistent with a looser structure being present in the ternary complex compared with the binary complexes.

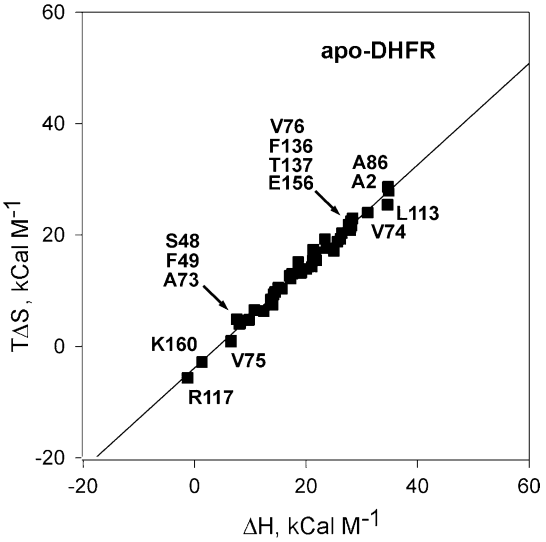


**Figure 5.** Plot of $\Delta H$ *versus* $T\Delta S$ for the amide NH exchange of residues in apo-DHFR.

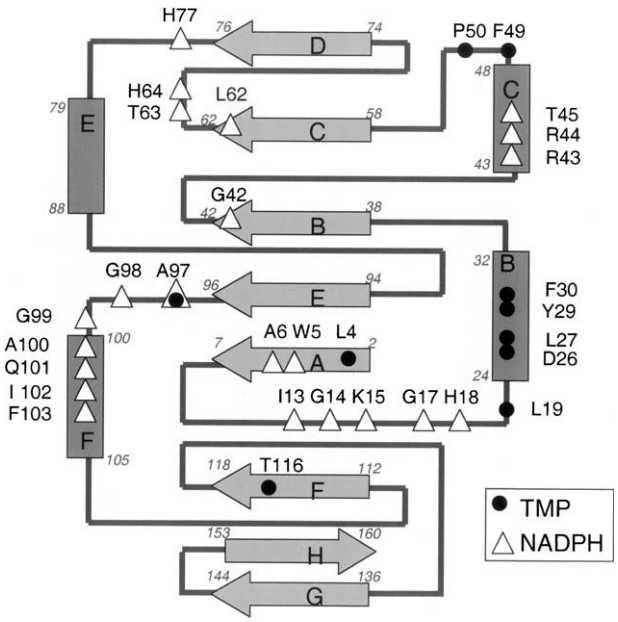


**Figure 6.** A diagram of the secondary structure elements in DHFR showing the eight β-strands (A, residues 2–7; B, 38–42; C, 58–62; D, 74–76; E 94–96; F, 112–118; G, 136–144; and H, 153–160) and the four α-helices (B, residues 24–33; C, 43–48; E, 79–88; and F, 100–105). Filled circles denote the residues that interact with TMP and open triangles denote those residues that interact with NADPH.

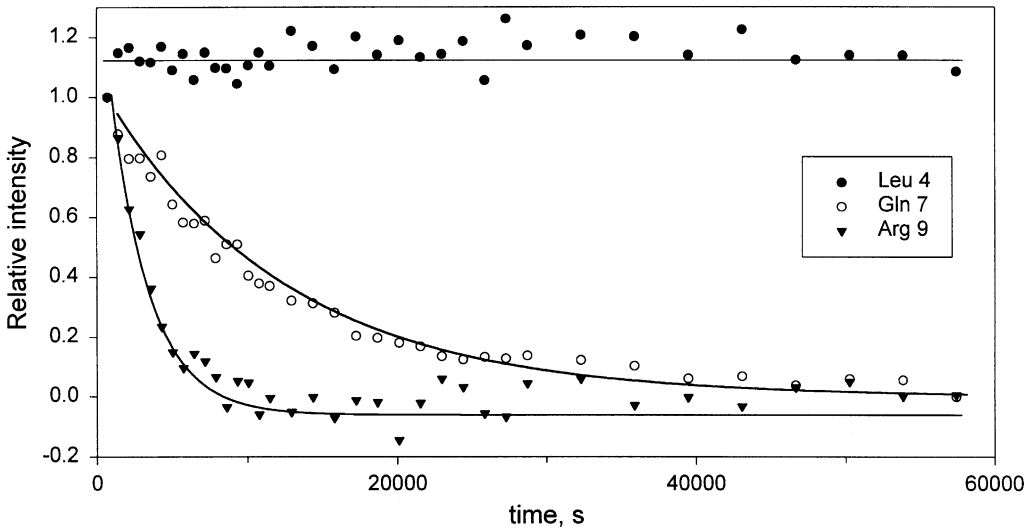


**Figure 7.** Illustrative decays of the signal intensities for three amide NH protons in the DHFR.TMP complex (prepared with non-MET-θ DHFR in the absence of excess ligand) that exchange with different rates.

## Materials and Methods

### Sample preparation

*L. casei* DHFR was expressed in *Escherichia coli* containing the *L. casei* DHFR gene and the protein was isolated and purified as described.[43,44] The enzyme concentration was 0.7 mM for the exchange experiments and up to 4 mM for the assignment studies. The freeze-dried samples were taken up either in $^2H_2O$ (exchange experiments) or in 90% $H_2O$/10% $^2H_2O$ (assignment experiments). Ligands (NADPH, $NADP^+$, folinic acid and TMP) were obtained from Sigma and were used without further purification. Samples of the complexes for the H/D experiments (DHFR.TMP, DHFR.NADPH, DHFR.$NADP^+$, DHFR.folinic acid, DHFR.TMP.$NADP^+$, DHFR.TMP.NADPH and DHFR.folinic acid.NADPH) in the presence of excess ligands were prepared as follows. Protein samples in 50 mM potassium phosphate ($pH^*$ = 6.5), 100 mM KCl, solutions were freeze-dried as aliquots to prepare 0.4 ml samples of 0.7 mM apo-DHFR. Freeze-dried aliquots of the ligands were prepared from pH-adjusted $H_2O$ solutions. The ligands were taken up in $^2H_2O$ and then added to aliquots of the apo-DHFR. In all cases, the excess ligand concentration was at least 400 times greater than the $K_d$: the relevant binding constants are large ($K_d$ values in the range $10^{-5}$–$10^{-10}$ M) and these high excess ligand concentrations ($1\times10^{-3}$–$10\times10^{-3}$ M free ligand) will result in essentially complete protein coverage.

For the higher pH experiments, apo-DHFR was adjusted to pH 7.5 by adding microliter amounts of concentrated NaOH or HCl solutions before freeze-drying.

The complexes containing NADPH, TMP and folinic acid were prepared using DHFR with an additional N-terminal methionine residue, while those with TMP/$NADP^+$ contained non-*N*-Met DHFR: the stability of the *N*-Met form is slightly greater than the non *N*-Met form (see Tables 1 and 2) and this was allowed for by using the relevant control samples in the subtractions used to obtain the $\Delta\Delta G_o$ values.

### NMR experiments

All spectra were collected on Varian UNITY, UNITY plus and INOVA spectrometers equipped with *z*-gradient triple-resonance probes operating at 500 MHz and 600 MHz ($^1H$ frequency) as described.[45] Amide proton exchange rates were determined in a series of $^1H$–$^{15}N$ HSQC spectra recorded as pseudo-3D experiments. To evaluate the extent of the protection of the amide protons quantitatively, rates of the H/D were measured from the time-course of the NH peak intensities in pseudo-3D experiments, where the first two dimensions are from the $^1H$ and $^{15}N$ resonances in the HSQC experiment and the third dimension is time, starting from the beginning of the experiment (after dissolving the freeze-dried samples in $^2H_2O$). Figure 7 illustrates the signal intensity decays for three amide protons that exchange with different rates in the DHFR.TMP binary complex at 15 °C. Acquisition of the first spectrum was usually started ~10 min after dissolving the protein sample in $^2H_2O$. The total acquisition time was between 16 and 20 h. Typically, 60 2D HSQC planes were collected over this time, giving time steps every 20 min. In some experiments, longer accumulation times (1–2 h) were used for later-time points. All spectra were processed with NMRPipe software,[46] and visualised with NMRDraw, XEASY[47] or Sparky†.

### NMR signal assignments in series of DHFR complexes

Signal assignments in the binary complex DHFR.TMP and the ternary complex DHFR.TMP.NADPH (BioMagRes Bank accession number 5396) are published.[34,48] Assignments of NH signals in apo-DHFR, DHFR.NADPH, DHFR.$NADP^+$, DHFR.TMP.$NADP^+$, DHFR.folinic acid and DHFR.folinic acid.NADPH were based on analysis of characteristic patterns of NOEs in NOESY-HSQC spectra recorded at 15 °C and/or 35 °C as described (being submitted to BioMagRes Bank).[44] For apo-DHFR, some of the signals in the HSQC are very broad and it was not possible to obtain good 3D data to

† http://www.cgl.ucsf.edu/home/sparky/

make the assignments. The signals were sharpened by titrating the sample with a weakly binding ligand, *p*-aminobenzoyl glutamate ($K_d \sim 10^{-3}$ M); the signals from this complex were then assigned and the assignments extrapolated back to the apo-DHFR spectrum. For the exchange experiments, in all the complexes, the cross-peaks remaining in the HSQC spectra after dissolving the samples in $^2H_2O$ were assigned by comparisons with spectra recorded on samples in $H_2O$. Assignments of amide $^1H$ and $^{15}N$ signals at various temperatures were achieved using superimposition of a series of HSQC spectra recorded over the temperature range 5–20 °C.

### Theoretical background to hydrogen/deuterium exchange

A structurally protected amide hydrogen atom exchanges with deuterium from the solvent according to the following general scheme:[49,50]

$$\text{Closed} - \text{NH} \underset{k_{cl}}{\overset{k_{op}}{\rightleftarrows}} \text{Open} - \text{NH} \xrightarrow{k_{int}} \text{Open} - \text{ND}$$

where $k_{op}$ and $k_{cl}$ are the rate constants for the opening and closing events involved in the hydrogen exchange and $k_{int}$ is the intrinsic rate constant of exchange for the amide hydrogen in the unfolded (random coil) state. The equilibrium constant for the opening/closing equilibrium $K_o$ is given by $K_o = k_{op}/k_{cl}$. In the case of an EX2 mechanism,[51] which is commonly accepted for slow exchange of protein amide protons under acidic pH conditions, $k_{cl} >> k_{int}$ and the observed rate constant of the exchange process is given by $k_{obs} = K_o k_{int}$. The ratio $k_{int}/k_{obs}$ (i.e. $1/K_o$) is defined by Molday and co-workers[52] as the amide protection factor *PF*, and reflects how well an amide hydrogen atom is protected by the protein tertiary structure from being exchanged with water. The terms *PF* and $K_o$ are related to the change of free energy of the opening/closing equilibrium:

$$\Delta G_o = -RT \ln K_o = RT \ln PF \quad (1)$$

In considering the influence of ligand binding on amide protection factors, we can introduce the ligand-induced protection factor, *LPF*:

$$LPF = \frac{PF^{\text{complex}}}{PF^{\text{apo}}} = \frac{k_{obs}^{\text{apo}}}{k_{obs}^{\text{complex}}} \quad (2)$$

The *LPF* is related to difference in free energy for the opening/closing equilibrium, $\Delta\Delta G_o^{\text{complex–apo}}$, between the protein–ligand complex and the unliganded protein:

$$\Delta\Delta G_o^{\text{complex–apo}} = \Delta G_o^{\text{complex}} - \Delta G_o^{\text{apo}}$$

$$= RT(\ln PF^{\text{complex}} - \ln PF^{\text{apo}}) = RT \ln LPF \quad (3)$$

Values of *LPF* reflect the contributions of the bound ligand to the overall structural protection of the amide hydrogen atom. The ligand can contribute to increasing or decreasing the structural protection of an amide NH hydrogen atom by changing the free energy of the closed state and/or by changing the energy of the opened state of each individual amide hydrogen atom (see Figure 8). The above determination of free energy changes from analysis of NH exchange rates is valid only under conditions where the EX2 mechanism ($k_{cl} >> k_{int}$) can be applied. In apo-DHFR and its complexes with TMP and TMP.NADPH, where the pH-dependence of the NH exchange has been measured (see Results), all of the NH protons measured increased their exchange rates on changing the pH from 6.5 to 7.5, as would be expected for the EX2 mechanism. This is not surprising, since under the conditions used here (pH 6.5, 15 °C and in the absence of denaturants) most amide NH protons would be expected to exchange *via* an EX2 mechanism.[52,53]

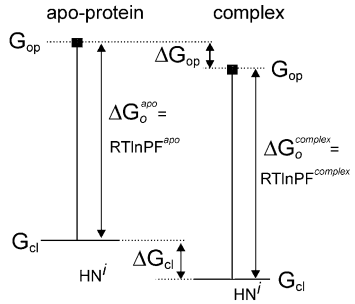


**Figure 8.** Energy diagram illustrating the meaning of $\Delta G_o = G_o^{\text{apo}} - G_o^{\text{complex}}$. The differences in free energies of the opened states ($G_{op}^{\text{apo}} - G_{op}^{\text{complex}}$) and the closed states ($G_{cl}^{\text{apo}} - G_{cl}^{\text{complex}}$) determine the $\Delta G_o$ value between apo-DHFR and its complex.

### Hydrogen to deuterium exchange rates and determination of protection factors

Signal intensities in the HSQC spectra were calculated using non-linear fitting of Gaussian-lineshape-processed NMR spectra using the nLinLS procedure from the NMRPipe package.[46] Peak areas obtained at the different time-points were fit to either two-parameter or three-parameter exponential decay functions to yield exchange rates (see Figure 7), calculation subroutines being coded in the RelaxFit program written in-house.[45] Errors in measured $k_{obs}$ values were estimated from their standard deviations obtained in the non-linear fitting.

An EX2 mechanism for H/D was assumed to be valid at pH* 6.5 throughout the whole experimental temperature range. Protection factors *PF* for the individual amide hydrogen atoms were calculated as ratios of intrinsic ($k_{int}$) and observed ($k_{obs}$) exchange rate constants.[54] Site-specific values $k_{int}$ were calculated as a sum of acid ($k_{acid}$), base ($k_{base}$) and water catalysed ($k_{water}$) rate constants at various temperatures, as described.[55]

Values of protection factors ($k_{int}/k_{obs} = 1/K_o$) were converted to the apparent values of free energy of the opening/closing process ($\Delta G_o$) using equation (1): these values are reported in Tables 1 and 2 for apo-DHFR and its ligand complexes. For very slowly exchanging residues, where the rate constants could not be determined accurately, their values of log($k$) were assumed to be equal to log($k_{min}$) − 1, where $k_{min}$ is the smallest but still measurable rate constant.

### Enthalpies and entropies for hydrogen exchange processes

Processes of protein opening are accompanied by breaking and re-establishing of numerous interactions. It is well known that the enthalpy and entropy changes of such processes are strongly temperature-dependent,[56,57] and in many cases it is not easy to describe such dependencies in an exact mathematical form. Following approaches used in protein unfolding studies (applying

the Gibbs–Helmoltz equation as used for example by Fersht[58]), one can express the temperature-dependence of protection factors as:

$$RT \ln PF = \Delta G_o = \Delta H - T\Delta S$$
$$= \Delta C_p(T - T_h) - T\Delta S_{T_h} - T\Delta C_p \ln\left(\frac{T}{T_h}\right) \quad (4)$$

where $T_h$ is the temperature at which $\Delta H = 0$. This equation can be re-written in a form that is more convenient for subsequent fitting of experimental data:

$$R \ln PF = \Delta C_p \left[1 - \frac{T_h}{T} + \ln\left(\frac{T_h}{T}\right)\right] - \Delta S_{T_h} \quad (5)$$

This equation is similar to one obtained previously by Sadqi and co-workers using a statistical thermodynamic approach.[16]

The experimentally measured protection factors at different temperatures can be fit to equation (5) by assuming that the heat capacity changes $\Delta C_p$ between closed and opened protein forms are independent of temperature (this assumption has been used, for instance, in studies of breaking of hydrophobic interactions[57]).

In order to determine the enthalpies and entropies, measurements of H/D rates were carried out at four different temperatures between 5 °C and 20 °C. Protection factors were calculated for each temperature and then fit to equation (5) by a non-linear regression method using the Levenberg–Marquardt algorithm,[59] with the protection factors and their standard deviations both being used in the fitting. The most reliable results were obtained for residues having protection factors measured at four different temperatures. Values of $\Delta C_p$, $T_h$ and $\Delta S_{Th}$ were obtained from the fitting (with standard deviations being obtained in cases where more than three temperature points were available). Values of $\Delta H$ and $\Delta S$ were calculated using equation (4), and the results are presented in Table 3 and Figure 5.

## Acknowledgements

The NMR measurements were carried out at the MRC Biomedical NMR Centre, NIMR, Mill Hill. We thank Geoff Kelly for help with the NMR measurements of H/D rates, Tom Frenkiel and Nigel Birdsall for useful discussions, and John McCormick for expert technical assistance. This research was supported by a Wellcome Trust Collaborative Research Initiative Grant 060140, and a grant from the Russian Foundation for Basic Research. V.I.P. is an International Scholar of the Howard Hughes Medical Institute.

## Supplementary Data

Supplementary data associated with this article can be found, in the online version, at doi:10.1016/j.jmb.2005.11.084

## References

1. Loh, S. N., Prehoda, K. E., Wang, J. & Markley, J. L. (1993). Hydrogen exchange in unligated and ligated staphylococcal nuclease. *Biochemistry*, **32**, 11022–11028.
2. Roder, H. (1989). Structural characterization of protein folding intermediates by proton magnetic resonance and hydrogen exchange. *Methods Enzymol.* **176**, 446–473.
3. Delepierre, M., Dobson, C. M., Selevarajah, S., Wedin, R. E. & Poulsen, F. M. (1983). Correlation of hydrogen exchange behaviour and thermal stability of lysozyme. *J. Mol. Biol.* **168**, 687–692.
4. Wüthrich, K., Wagner, G., Richarz, R. & Braun, W. (1980). Correlations between internal mobility and stability of globular proteins. *Biophys. J.* **32**, 549–558.
5. Wagner, G. & Wüthrich, K. (1979). Correlation between the amide proton exchange rates and the denaturation temperatures in globular proteins related to the basic pancreatic trypsin inhibitor. *J. Mol. Biol.* **130**, 31–37.
6. Wagner, G. & Wüthrich, K. (1979). Structural interpretation of the amide proton exchange in the basic pancreatic trypsin inhibitor and related proteins. *J. Mol. Biol.* **134**, 75–94.
7. Englander, S. W., Englander, J. J., McKinnie, R. E., Ackers, G. K., Turner, G. J., Westrick, J. A. & Gill, S. J. (1992). Hydrogen exchange measurement of the free energy of structural and allosteric change in hemoglobin. *Science*, **256**, 1684–1687.
8. Casares, S., Sadqi, M., Lopez-Mayorga, O., Martinez, F. & Conejero-Lara, F. (2003). Structural co-operativity in the SH3 domain studied by site-directed mutagenesis and amide hydrogen exchange. *FEBS Letters*, **539**, 125–130.
9. Jeng, M-F. & Englander, S. W. (1991). Stable submolecular folding units in a non-compact form of cytochrome *c*. *J. Mol. Biol.* **221**, 1045–1061.
10. Morozova, L. A., Haynie, D. T., Arico-Muendel, C., Van Dael, H. & Dobson, C. M. (1995). Structural basis of the stability of a lysozyme molten globule. *Nature Struct. Biol.* **2**, 871–875.
11. Clarke, J. & Fersht, A. R. (1996). An evaluation of the use of hydrogen exchange at equilibrium to probe intermediates on the protein folding pathway. *Fold. Des.* **1**, 243–254.
12. Hilser, V. J. & Freire, E. (1996). Structure-based calculation of the equilibrium folding pathway of proteins. Correlation with hydrogen exchange protection factors. *J. Mol. Biol.* **262**, 756–778.
13. Hilser, V. J. & Freire, E. (1997). Predicting the equilibrium protein folding pathway: structure-based analysis of staphylococcal nuclease. *Proteins: Struct. Funct. Genet.* **27**, 171–183.
14. Hilser, V. J., Dowdy, D., Oas, T. G. & Freire, E. (1998). The structural distribution of co-operative interactions in proteins: analysis of the native state ensemble. *Proc. Natl Acad. Sci. USA*, **95**, 9903–9908.
15. Sadqi, M., Casares, S., Abril, M. A., Lopez-Mayorga, O., Conejero-Lara, F. & Freire, E. (1999). The native state conformational ensemble of the SH3 domain from alpha-spectrin. *Biochemistry*, **38**, 8899–8906.
16. Sadqi, M., Casares, S., Lopez-Mayorga, O. & Conejero-Lara, F. (2002). The temperature dependence of the hydrogen exchange in the SH3 domain of α-spectrin. *FEBS Letters*, **527**, 86–90.

17. Englander, S. W. (2000). Protein folding intermediates and pathways studied by hydrogen exchange. *Annu. Rev. Biophys. Biomol. Struct.* **29**, 213–238.
18. Bai, Y., Sosnick, T. R., Mayne, L. & Englander, S. W. (1995). Protein folding intermediates: native state hydrogen exchange. *Science*, **269**, 192–197.
19. Chamberlain, A. K., Handel, T. M. & Marqusee, S. (1996). Detection of rare partially folded molecules in equilibrium with the native conformation of RNaseH. *Nature Struct. Biol.* **3**, 782–787.
20. Fuentes, E. J. & Wand, A. J. (1998). Local stability and dynamics of Apocytochrome $b_{562}$ examined by the dependence of hydrogen exchange on hydrostatic pressure. *Biochemistry*, **37**, 9877–9883.
21. Clarke, J. & Fersht, A. R. (1996). An evaluation of the use of hydrogen exchange at equilibrium to probe intermediates on the protein folding pathway. *Fold. Des.* **1**, 243–254.
22. Freire, E. (1999). The propagation of binding interactions to remote sites in proteins: analysis of the binding of the monoclonal antibody D1.3 to lysozyme. *Proc Natl Acad. Sci. USA*, **96**, 10118–10122.
23. Freire, E. (2000). Can allosteric regulation be predicted from structure? *Proc. Natl Acad. Sci. USA*, **97**, 11680–11682.
24. Pan, H., Lee, J. C. & Hilser, V. (2000). Binding sites in *E. coli* dihdrofolate reductase communicate by modulating the conformational ensemble. *Proc. Natl Acad. Sci. USA*, **97**, 12020–12025.
25. Williams, D. H., Stephens, E. & Zhou, M. (2003). Ligand binding energy and catalytic efficiency from improved packing with receptors and enzymes. *J. Mol. Biol.* **329**, 389–399.
26. Williams, D. H., Stephens, E. & Zhou, M. (2003). How can enzymes be so efficient? *Chem. Commun.* 1973–1976.
27. Williams, D. H., Stephens, E., O'Brien, D. P. & Zhou, M. (2004). Understanding non-covalent interactions: ligand binding energy and catalytic efficiency from ligand-induced reductions in motion within receptors and enzymes. *Angew. Chem. Int. Ed.* **43**, 6596–6616.
28. Kalodimos, C. G., Boelens, R. & Kaptein, R. (2002). A residue specific view of the association and dissociation pathway in protein–DNA recognition. *Nature Struct. Biol.* **9**, 193–197.
29. Kalodimos, C. G., Boelens, R. & Kaptein, R. (2004). Towards an integrated model of protein–DNA recognition as inferred from NMR studies on the *Lac* repressor system. *Chem. Rev.* **104**, 3567–3586.
30. Feeney, J. (2000). NMR studies of ligand binding to dihydrofolate reductase. *Angew. Chem. Int. Ed.* **39**, 290–312.
31. Baccanari, D. P., Daluge, S. & King, R. W. (1982). Inhibition of dihydrofolate reductase: effect of reduced nicotinamide adenine dinucleotide phosphate on the selectivity and affinity of diaminobenzylpyrimidines. *Biochemistry*, **21**, 5068–5075.
32. Birdsall, B., Hyde, E. I., Burgen, A. S. V., Roberts, G. C. K. & Feeney, J. (1981). Negative cooperativity between folinic acid and coenzyme in their binding to *L. casei* dihydrofolate reductase. *Biochemistry*, **20**, 7186–7195.
33. Andrews, J., Fierke, C. A., Birdsall, B., Ostler, G., Feeney, J., Roberts, G. C. K. & Benkovic, S. J. (1989). A kinetic study of wild type and mutant dihydrofolate reductases. *Biochemistry*, **28**, 5743–5750.
34. Polshakov, V. I., Smirnov, E. G., Birdsall, B., Kelly, G. & Feeney, J. (2002). Letter to the editor: NMR-based solution structure of the complex of *Lactobacillus casei* dihydrofolate reductase with trimethoprim and NADPH. *J. Biomol. NMR*, **24**, 67–70.
35. Milne, J. S., Xu, Y., Mayne, L. C. & Englander, S. W. (1999). Experimental study of the protein folding landscape: unfolding reactions in cytochrome *c*. *J. Mol. Biol.* **290**, 811–822.
36. Dunitz, J. D. (1995). Win some, lose some: enthalpy–entropy compensation in intermolecular interactions. *Chem. Biol.* **11**, 709–712.
37. Searle, M. S., Forster, M. J., Birdsall, B., Roberts, G. C. K., Feeney, J., Cheung, H. T. A. *et al*. (1988). Dynamics of trimethoprim bound to dihydrofolate reductase. *Proc. Natl Acad. Sci. USA*, **85**, 3787–3791.
38. Polshakov, V. I., Birdsall, B. & Feeney, J. (1999). Characterisation of rates of ring flipping in trimethoprim and its ternary complexes with *Lacotobacilus casei* dihydrofolate reductase and coenzyme analogues. *Biochemistry*, **38**, 15962–15969.
39. Makhatadze, G. I. & Privalov, P. L. (1993). Contribution of hydration to protein folding thermodynamics. I. The enthalpy of hydration. *J. Mol. Biol.* **232**, 639–659.
40. Makhatadze, G. I. & Privalov, P. L. (1996). On the entropy of protein folding. *Protein Sci.* **5**, 507–510.
41. Gomez, J., Hilser, V. J., Xie, D. & Freire, E. (1995). The heat capacity of proteins. *Proteins: Struct. Funct. Genet.* **22**, 404–412.
42. Birdsall, B., Burgen, A. S. V. & Roberts, G. C. K. (1980). Binding of coenzyme analogues to *Lactobacillus casei* dihydrofolate reductase: binary and ternary complexes. *Biochemistry*, **19**, 3723–3731.
43. Dann, J. G., Ostler, G., Bjur, R. A., King, R. W., Scudder, P., Turner, P. C. *et al*. (1976). Large-scale purification and characterization of dihydrofolate reductase from a methotrexate-resistant strain of *Lactobacillus casei*. *Biochem J.* **157**, 559–571.
44. Andrews, J., Clore, G. M., Davies, R. W., Gronenborn, A. M., Gronenborn, B., Kalderon, D. *et al*. (1985). Nucleotide sequence of the dihydrofolate reductase gene of methotrexate-resistant *Lactobacillus casei*. *Gene*, **35**, 217–222.
45. Polshakov, V. I., Birdsall, B., Frenkiel, T. A., Gargaro, A. R. & Feeney, J. (1999). Structure and dynamics in solution of the complex of *Lactobacillus casei* dihydrofolate reductase with the new lipophylic antifolate drug trimetrexate. *Protein Sci.* **8**, 467–481.
46. Delaglio, F., Grzesiek, S., Vuister, G. W., Zhu, G., Pfeifer, J. & Bax, A. (1995). NMRPipe: a multidimensional spectral processing system based on UNIX pipes. *J. Biomol. NMR*, **6**, 277–293.
47. Bartels, Ch., Xia, T.-H., Billeter, M., Güntert, P. & Wüthrich, K. (1995). The program XEASY for computer-supported NMR spectral analysis of biological macromolecules. *J. Biomol. NMR*, **5**, 1–10.
48. Martorell, G., Gradwell, M. J., Birdsall, B., Bauer, C. J., Frenkiel, T. A., Cheung, H. T. A. *et al*. (1994). Solution structure of bound trimethoprim in its complex with *Lactobacillus casei* dihydrofolate reductase. *Biochemistry*, **33**, 12416–12426.
49. Berger, A. & Linderstrom-Lang, K. (1957). Deuterium exchange of poly-DL-alanine in aqueous solution. *Arch. Biochem. Biophys.* **69**, 106–118.
50. Englander, S. W. & Kallenbach, N. R. (1984). Hydrogen exchange and structural dynamics of proteins and nucleic acids. *Quart. Rev. Biophys.* **16**, 521–655.
51. Hvidt, A. & Nielsen, S. O. (1966). Hydrogen exchange in proteins. *Advan. Protein Chem.* **21**, 287–386.

52. Ferraro, D. M., Lazo, N. D. & Robertson, A. D. (2004). EX1 hydrogen exchange and protein folding. *Biochemistry*, **43**, 587–594.
53. Dalby, P. A., Clarke, J., Johnson, C. M. & Fersht, A. R. (1998). Folding intermediates of wild-type and mutants of barnase. II. correlation of changes in equilibrium amide exchange kinetics with the population of the folding intermediate. *J. Mol. Biol.* **276**, 647–656.
54. Molday, R. S., Englander, S. W. & Kallen, R. G. (1972). Primary structure effects on peptide group hydrogen exchange. *Biochemistry*, **11**, 150–158.
55. Bai, Y., Milne, J. S., Mayne, I. & Englander, S. W. (1993). Primary structure effects on peptide group hydrogen exchange. *Proteins: Struct. Funct. Genet.* **17**, 75–86.
56. Privalov, P. L. & Gill, S. J. (1988). Stability of protein-structure and hydrophobic interaction. *Advan. Protein Chem.* **39**, 191–234.
57. Lee, B. (1994). Enthalpy–entropy compensation in the thermodynamics of hydrophobicity. *Biophys. Chem.* **51**, 271–278.
58. Fersht, A. (1999). Protein stability. In *Structure and Mechanism in Protein Science. A Guide to Enzyme Catalysis and Protein Folding* chap. 17, pp. 508–539, W.H. Freeman and Co., New York.
59. Press, W. H., Teukolsky, S. A., Vetterling, W. T. & Flannery, B. P. (1992). *Numerical recipes in FORTRAN* (2nd edit.) *The Art of Scientific Computing*, University Press, Cambridge, UK.
60. Kraulis, P. E. (1991). MOLSCRIPT: a program to produce both detailed and schematic plots of protein structures. *J. Appl. Crystallog.* **24**, 946–950.
61. Birdsall, B., Bevan, A. W., Pascuale, C., Roberts, G. C. K., Feeney, J., Gronenborn, A. & Clore, G. M. (1984). Multinuclear NMR characterization of two coexisting comformational states of the *Lactobacillus casei* dihydrofolate reductase-trimethoprim-$NADP^+$ complex. *Biochemistry*, **23**, 4733–4742.

***Edited by P. Wright***

*(Received 5 May 2005; received in revised form 24 November 2005; accepted 28 November 2005)*
Available online 15 December 2005